PHYSICAL REVIEW C **71**, 044902 (2005)

Formation of Hubble-like flow in little bangs

Mikołaj Chojnacki*
Institute of Physics, Świętokrzyska Academy, PL-25406 Kielce, Poland

Wojciech Florkowski†
Institute of Physics, Świętokrzyska Academy, PL-25406 Kielce, Poland and
Institute of Nuclear Physics, Polish Academy of Sciences, PL-31342 Kraków, Poland

Tamás Csörgö‡
MTA KFKI RMKI, H-1525 Budapest 114, Post Office Box 49, Hungary
(Received 5 November 2004; published 21 April 2005)

The dynamical appearance of scaling solutions in relativistic hydrodynamics is studied for boost-invariant, cylindrically symmetric systems. Such solutions reproduce key qualitative features of the blast-wave, Buda-Lund, and Cracow models, which in turn fit a broad set of data measured in ultrarelativistic heavy-ion collisions. Effects of a phase transition are taken into account by using a temperature-dependent speed of sound, inferred from a lattice QCD equation of state. The transverse flow may acquire the asymptotic Hubble form r/t within short evolution times, 7–15 fm, only if an initial pre-equilibrium transverse flow is present. The precise amount of the requisite pre-equilibrium flow is anticorrelated with the initial value of the central temperature.

DOI: 10.1103/PhysRevC.71.044902 PACS number(s): 25.75.Dw, 21.65.+f, 14.40.−n

I. INTRODUCTION

Hadronic data collected in the heavy-ion experiments at RHIC support the idea that the system formed in Au + Au collisions is highly thermalized and undergoes strong transverse and longitudinal expansion [1]. Moreover, successful parameterizations of the freeze-out process indicate that such expansion may be characterized by the Hubble law [2–4]. In the simplest form, used in cosmology, this law states the proportionality of the relative velocity of galaxies to their relative separation,

$$\mathbf{v} = H\mathbf{r}. \tag{1}$$

The constant of proportionality, or Hubble's constant H, is a function of time. In the Friedmann universe [5] as well as in analytic solutions of nonrelativistic fireball hydrodynamics [6], its value is

$$H = \frac{\dot{R}}{R}, \tag{2}$$

where the function $R(t)$ is in general a complicated function of time. In nuclear hydrodynamics, the Hubble law characterizes the fluid velocity distributions of the expanding matter; in cosmology the Hubble law characterizes the expansion of space. In nonrelativistic hydrodynamics, the scale parameter $R(t)$ depends on the initial conditions as well as on the equation of state, whereas in cosmology the time evolution of the scale parameter R depends not only on the initial conditions (flat, open, or closed universe) and the properties of matter (matter-dominated and radiation-dominated epoch) but also on the possible existence of dark energy and cosmological constants and the possible presence of an exponentially accelerating, inflatory period. At the end of the accelerating period, when $\dot{R} =$ constant, and $R \approx \dot{R}\,t$, the Hubble constant is simply the inverse of the lifetime, $H = 1/t$.

At the very end of the nuclear fireball explosion, the pressure decreases to vanishing values; hence the acceleration caused by pressure gradients becomes negligibly small. In this case, in analogy to the case observed in cosmology, we may expect that a simple form of the Hubble law connects the hydrodynamic four-velocity u^μ with the space-time position of the fluid element x^μ,

$$u^\mu = \frac{x^\mu}{\tau} = \frac{t}{\tau}\left(1, \frac{x}{t}, \frac{y}{t}, \frac{z}{t}\right). \tag{3}$$

The quantity τ in Eq. (3) is the proper time characterizing the freeze-out hypersurface,

$$\tau = \sqrt{t^2 - r^2 - z^2}, \quad r = \sqrt{x^2 + y^2}. \tag{4}$$

Clearly, the parametrization (3) and (4) makes sense in the space-time region defined by the condition $r^2 + z^2 < t^2$. In fact, the three-velocity field of the form

$$\mathbf{v} = \left(\frac{x}{t}, \frac{y}{t}, \frac{z}{t}\right), \tag{5}$$

following directly from Eq. (3), appears very often in the analysis of the hydrodynamic equations applied to describe hadronic or nuclear collisions. In this context it is called the *scaling solution* [7–12]. In particular, for the boost-invariant systems the longitudinal velocity must be of the form $v_z = z/t$, which is a direct consequence of Lorentz symmetry [11,13–17]. It is often believed that during the initial pre-equilibrium period of high-energy nuclear collisions, no significant transverse flow is generated. (For recent reviews of the hydrodynamic description of relativistic heavy-ion collisions see, e.g.,

*Electronic address: chojnacki_mikolaj@tlen.pl
†Electronic address: Wojciech.Florkowski@ifj.edu.pl
‡Electronic address: csorgo@sunserv.kfki.hu

Refs. [18–21].) In such a case, the transverse fluid velocity builds up during the hydrodynamic evolution of the system [12] and the scaling form in the transverse direction, $v_r = r/t$, may be reached only for sufficiently large times (with details depending on the equation of state and initial conditions). Similar features also characterize a spherically symmetric expansion of the system being initially at rest. In this case, the radial flow is formed by the outward action of the pressure gradient, and both the analytic [10,22] and numerical [10,12] calculations show that Eq. (3) is the asymptotic solution if the sound velocity satisfies the condition $c_s^2 \leqslant 1/5$. For more general cases various numerical calculations [12,19,23] show that the transverse-velocity profiles approach a linear dependence characterized by Eq. (1).

Recently, there is a revived theoretical interest in finding exact solutions of relativistic hydrodynamics. Bíró found an interesting solution, relevant for the case of a vanishing speed of sound, which interpolates between an early Bjorken type of flow profile and the Hubble profile in the late period of the expansion [24,25]. New exact solutions of relativistic hydrodynamics were found, using more general equations of state, in the $(1 + 1)$-dimensional case [26] and in the $(1 + 3)$-dimensional case for axially symmetric [27,28] as well as for ellipsoidally symmetric expansions [29]. Although these solutions contain arbitrary scaling functions describing the rapidity profile, the flow profile in all of these works coincides with the Hubble law.

In view of the success of the fits [2,4,30,31] (which all indicate very strong transverse flows), one of the central issues is whether the times actually available in relativistic heavy-ion collisions are sufficient to allow for a dynamical development of such strong transverse flows, in particular, the scaling solutions corresponding to Eq. (3). The situation is especially intriguing for RHIC, where several measurements indicate an unexpected, rather short (about 6–15 fm) duration time for the collision process. For example, one finds $\tau \sim 10$ fm using the RHIC data in the relation $R_L(m_T) = \tau\sqrt{T_k/m_T}$ [32], which connects the longitudinal pion correlation radius R_L, the kinetic freeze-out temperature T_k, the evolution time τ, and the transverse mass of the pion pair m_T. The authors of Ref. [4] obtained only 6 fm for the effective duration of the hydrodynamic evolution in Au + Au collisions at RHIC.

These measurements, when interpreted with care, yield only the inverse of the (longitudinal) Hubble constant, which can be identified with the lifetime only if the scaling solution is assumed to be developed in the longitudinal direction. This situation is analogous to the estimate of the lifetime of the Universe: The inverse of the presently measured value of the Hubble constant yields an order-of-magnitude estimate of the lifetime, which has to be corrected for the effects of inflation and possible other acceleration periods. Similarly, in nuclear hydrodynamics, there is an initial longitudinal acceleration period; hence the estimated lifetimes should be interpreted only as (lower) limits on the total lifetime of the system [33,34].

Many hydrodynamic codes used to describe heavy-ion data show that the scaling solutions do not appear before the freeze-out of the system. However, such approaches assume commonly that the initial transverse flow is zero. An exception to this rule is the work by Kolb and Rapp [35], who consider the pre-equilibrium transverse flow, the presence of which improves the agreement of the model calculations with the data. Another important exception is a class of the nonrelativistic, self-similar solutions of the fireball hydrodynamics, which is by now solved completely in the ellipsoidally symmetric case for arbitrary initial sizes and expansion velocities of the principal axes of the expanding ellipsoids [36], arbitrary initial temperature profiles [37], and arbitrary (temperature-dependent) speed of sound [38].

In this paper we follow such ideas and assume that the elementary parton-parton collisions, leading to the thermalization of the system, lead also to collective behavior and development of the transverse flow already at the initial stage of the equilibrium hydrodynamic evolution at the time $t = t_0 \sim 1$ fm. For simplicity, we consider boost-invariant and cylindrically symmetric systems with the initial transverse flow defined by the formula

$$v_r^0 = v_r(t = t_0, r) = \frac{H_0 r}{\sqrt{1 + H_0^2 r^2}}. \tag{6}$$

The parameter H_0 in Eq. (6) may be interpreted as the Hubble constant that determines the magnitude of the initial transverse flow; in the range $r < 1/H_0$ the flow is well approximated by the linear function $v_r^0 \sim H_0 r$, whereas for $r > 1/H_0$ the flow approaches the speed of light, a boundary condition frequently assumed in hydrodynamic equations for large values of r [12]. Also, if Eq. (6) is specified on a hypersurface corresponding to a constant proper time, it coincides with the Hubble law of Eq. (3).

By varying the value of H_0 we control the amount of the initial transverse flow that may possibly develop into the scaling form (5). We note that in the scaling solution (5) the role of the Hubble constant is played by the inverse of the time coordinate t. This means that by setting $H_0 = 1/t_0 = 1\,(\text{fm})^{-1}$ we assume that the initial flow is already very close to the scaling form at t_0. In this particular case the question arises whether the flow remains close to the scaling form in the subsequent time evolution of the system.

A few comments are now in order. Following the conventional hydrodynamic approach [12], we specify the initial conditions at a constant time, $t_0 = 1$ fm, and search for the solutions that are regular functions of t and r in the region $t > t_0, r > 0$. In this case, at a given value of time t, the scaling solution cannot hold for arbitrary large values of r, since this would yield flow velocities larger than the speed of light, and also the initial condition deviates from Eq. (1) for large values of the transverse radius. Hence, in our analysis we search for solutions of the hydrodynamic equations that yield the flow profiles possibly close to the scaling solution in the region $r < t$. In a separate paper we intend to explore a different type of the initial conditions, which are specified at a fixed value of the proper time and lead, in certain special cases, to the exact solutions given in Refs. [28,29]. We also note that in view of the recent BRAHMS data [39,40] describing rapidity dependence of hadron production, the boost-invariant approach assumed in the present calculation may be appropriate only if limited to the rapidity range $-1 < y < 1$.

II. CHARACTERISTIC FORM OF THE HYDRODYNAMIC EQUATIONS

In this section we introduce the basic notation and rewrite the hydrodynamic equations in a form convenient for numerical calculations. We follow closely the method introduced by Baym *et al.* [12]. We restrict our considerations to the systems with zero net baryon density, which is a good approximation for description of the central rapidity region at RHIC energies. (Thermal analysis of the ratios of hadron multiplicities indicates that the baryon chemical potential at RHIC energies is about 30 MeV; i.e., it is much smaller than the corresponding temperature of about 170 MeV [4,41,42].) In this case the hydrodynamic equations have the form

$$u^\mu \partial_\mu (T\, u^\nu) = \partial^\nu T, \tag{7}$$

$$\partial_\mu (\sigma u^\mu) = 0, \tag{8}$$

where T is the temperature, σ is the entropy density, and $u^\mu = \gamma\,(1, \mathbf{v})$ is the hydrodynamic four-velocity (with $\gamma = 1/\sqrt{1-v^2}$). Equation (7) follows from the relativistic Euler equation for perfect fluids and vanishing baryon chemical potential, whereas Eq. (8) represents entropy conservation (the adiabaticity of the flow). Since T is the only independent thermodynamic variable, all other thermodynamic quantities can be obtained from the equation of state $P\,(T)$, connecting pressure P with the temperature T. With the help of the thermodynamic relations

$$d\varepsilon = T d\sigma, \qquad dP = \sigma dT, \qquad w = \varepsilon + P = T\sigma, \tag{9}$$

other thermodynamic quantities, such as the energy density ε or the enthalpy density w, can be obtained. In addition, the equation of state allows us to calculate the sound velocity

$$c_s^2 = \frac{\partial P}{\partial \varepsilon} = \frac{\sigma}{T}\frac{\partial T}{\partial \sigma}. \tag{10}$$

Equation (8) and the spatial components of Eq. (7) may be rewritten for boost-invariant systems with cylindrical symmetry as

$$v_r \frac{\partial \ln T}{\partial t} + \frac{\partial \ln T}{\partial r} + \frac{\partial \alpha}{\partial t} + v_r \frac{\partial \alpha}{\partial r} = 0, \tag{11}$$

$$\frac{\partial \ln \sigma}{\partial t} + v_r \frac{\partial \ln \sigma}{\partial r} + v_r \frac{\partial \alpha}{\partial t} + \frac{\partial \alpha}{\partial r} + \frac{1}{t} + \frac{v_r}{r} = 0, \tag{12}$$

where α is the transverse rapidity of the fluid defined by the condition $v_r = \tanh\alpha$. The longitudinal component has the well-known boost-invariant form $v_z = z/t$ [11].

By introducing the potential $\Phi\,(T)$ defined by the differentials

$$d\Phi = \frac{d \ln T}{c_s} = c_s d \ln \sigma, \tag{13}$$

and by using the two functions $a_\pm$ defined by the formula

$$a_\pm = \exp\left(\Phi \pm \alpha\right), \tag{14}$$

Eqs. (11) and (12) may be cast into the characteristic form [12]

$$\frac{\partial}{\partial t} a_\pm(t,r) + \frac{v_r \pm c_s}{1 \pm v_r\, c_s}\frac{\partial}{\partial r} a_\pm(t,r) + \frac{c_s}{1 \pm v_r\, c_s}\left(\frac{v_r}{r} + \frac{1}{t}\right) a_\pm(t,r) = 0 \tag{15}$$

If the functions $a_\pm$ are known, the potential Φ may be calculated from the formula

$$\Phi = \frac{1}{2}\ln(a_+ a_-), \tag{16}$$

and the velocity is obtained from the equation

$$v_r = \frac{a_+ - a_-}{a_+ + a-}. \tag{17}$$

Knowledge of the function $c_s(T)$ allows us, by the integration of Eq. (13), to determine Φ as a function of the temperature; this function will later be called Φ_T. However, to get a closed system of equations for a_+ and a_-, we have to invert this relation and obtain T as a function of Φ; this function will later be called T_Φ. In this way, the sound velocity may be expressed in terms of the functions a_+ and a_-,

$$c_s = c_s\left[T_\Phi\left(\frac{1}{2}\ln(a_+ a_-)\right)\right], \tag{18}$$

and Eqs. (15) may be solved numerically.

III. TEMPERATURE DEPENDENT SOUND VELOCITY

In our numerical calculations we take into account the temperature dependence of the sound velocity. In this way, we generalize the approach of Ref. [12], where Eqs. (15)–(17) were solved numerically only in the case $c_s^2 = 1/3$. The results of different model calculations of the sound velocity, which may serve as input for the hydrodynamic calculations, are presented in Fig. 1(a). The solid line (denoted as "lattice I") is a result of Mahonty and Alam [43], who compiled the lattice results obtained by Karsch [44] to get $c_s(T)$ from the temperature dependence of the energy density. The long-dashed line (denoted as "lattice II") shows the result of the lattice QCD calculations by Szabó and Tóth [45]. A sudden but smooth change of the sound velocity in the small temperature range around $T = T_c$, as observed in the lattice calculations [see Fig. 1 (a)] indicates a rapid crossover from a hadron gas to a quark-gluon plasma phase. Above the critical temperature ($T \gg T_c$) the sound velocity approaches the limit valid for massless particles, $c_s^2 = 1/3$, whereas below the phase transition ($T \ll T_c$) the sound velocity is much smaller, being close to the value obtained for the case of a noninteracting gas of hadron resonances.

The hadron-gas result shown in Fig. 1(a) was obtained in a calculation that uses recent fits to the meson and baryon mass spectra [46–48] denoted in the following by $\rho_M(m)$ and $\rho_B(m)$. One possible parametrization of the spectra [47], which directly reveals their exponential growth, as suggested long ago by Hagedorn [49], is as follows:

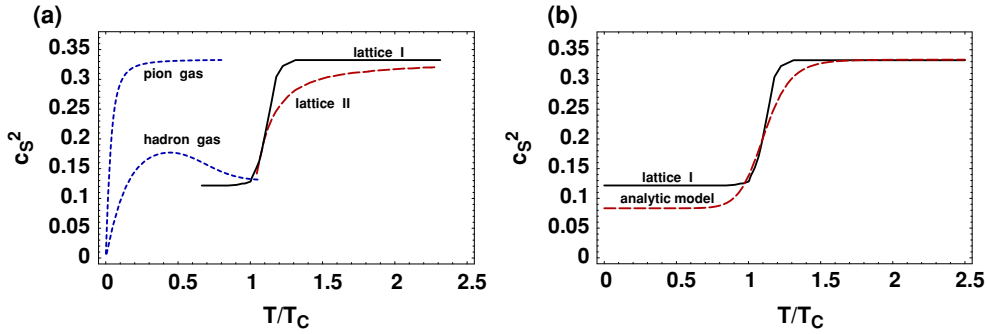

FIG. 1. (Color online) (a) Temperature dependence of the sound velocity as obtained from different theoretical models described in the text. (b) Sound velocity used in this calculation: The solid line describes the lattice result (i.e., the function "lattice I") from (a) extrapolated to low temperatures, whereas the dashed line describes the analytic model defined by Eq. (21).

$$\begin{aligned} \rho_M(m) &= a_M \exp(m/T_M), & a_M &= 4.41\,\mathrm{GeV}^{-1}, \\ T_M &= 311\,\mathrm{MeV}, & \rho_B(m) &= a_B \exp(m/T_B), \\ a_B &= 0.11\,\mathrm{GeV}^{-1}, & T_B &= 186\,\mathrm{MeV}. \end{aligned} \tag{19}$$

With the help of the mass distributions (19), we calculate the entropy density of the hadron gas as a sum over contributions from all known hadronic states from the formula

$$\sigma(T) = \frac{1}{2\pi^2}\int_{m_{\mathrm{pion}}}^{M_{\mathrm{mesons}}^{\max}} \rho_M(m) m^3 K_3\left(\frac{m}{T}\right) dm + \frac{2}{2\pi^2}\int_{m_{\mathrm{nucleon}}}^{M_{\mathrm{baryons}}^{\max}} \rho_B(m) m^3 K_3\left(\frac{m}{T}\right) dm. \tag{20}$$

The sound velocity of the hadron gas then follows directly from the use of Eq. (20) in (10). Equation (20) is valid in the case of zero baryon chemical potential and the factor 2 in the second term accounts for antibaryons. The effects of the quantum statistics (Bose-Einstein or Fermi-Dirac) are neglected in Eqs. (20), because they are known to be small, being of the order of 20% or less for reasonable range of the temperatures [8]. To match our hadron-gas calculation with the lattice data we assumed that the critical temperature is 170 MeV. The upper limits of the integrations in (20) are $M_{\mathrm{mesons}}^{\max} = 2.3$ GeV for mesons and $M_{\mathrm{baryons}}^{\max} = 1.8$ GeV for baryons. These limits are determined by the range where the fit (19) works well [48]; for higher masses, the spectra saturate owing to the lack of data.

For comparison, in Fig. 1(a) we show the speed of sound obtained in a similar calculation where only the massive pions are included. The speed of sound in a pion gas quickly reaches the limiting value of $1/\sqrt{3}$, which may be compared with the nonmonotonic behavior of c_s in the gas of resonances. Similar behavior of the speed of sound in the gas of resonances was also found in the case with nonzero baryon density [50]. It is interesting to note that the lattice data agree with the hadron-gas calculation close to the phase transition region if we assume $T_c \sim 170$ MeV. Moreover, the speed of sound in the hadron resonance gas below the critical temperature is found to be significantly smaller than $1/\sqrt{3}$, which is the limit of a massless ideal relativistic gas used in the bag model type of the equations of state. As the hydrodynamic equations describe the properties of matter through the equation of state, or more precisely through the speed of sound [8], such a decrease of the speed of sound in the hadron gas stage, compared to the massless pion gas limit, changes drastically the corresponding time evolution of the hydrodynamic solutions.

Although the calculations of the speed of sound shown in Fig. 1(a) are based on the observed hadron mass spectra below T_c and on the lattice QCD above T_c, they are still somewhat ambiguous and not completely satisfactory. For example, lattice QCD calculations below the critical temperature still yield pions that are too heavy, and we know that the value of the speed of sound is rather sensitive to pion mass. Moreover, even though the calculation based on the Hagedorn mass spectrum in the hadronic phase is more realistic than the lattice results in the low-temperature domain, it neglects the role of interactions among hadrons.

In this situation, we decided to use as the main input the equation of state (sound velocity) reported by Ref. [43], which is shown as "lattice I" in Fig. 1(a). This calculation is based on first principles and extends down to about 0.6 T_c (i.e., to the low-temperature region of about 100 MeV relevant for the discussions of kinetic freeze-out). In the actual calculation we extrapolate this result to even lower temperatures as shown in Fig. 1(b). We also use an analytic form of the function $c_s(T)$ that exhibits the main features observed in Fig. 1(a) and, at the same time, leads to the analytic expressions for the functions $\Phi_T(T)$ and $T_\Phi(\Phi)$. This function is defined by the formula

$$c_s(T) = \frac{1}{\sqrt{3}}\left[1 - \frac{1}{2}\left(\frac{1}{1+(T/\tilde{T})^{2n}}\right)\right]. \tag{21}$$

Using Eq. (21) one finds $c_s(T) = 1/\sqrt{3}$ for $T \gg \tilde{T}$ and $c_s(T) = 1/(2\sqrt{3})$ for $T \ll \tilde{T}$. A straightforward integration of Eq. (13) gives in this case

$$\Phi_T(T) = \frac{\sqrt{3}}{2n}\ln\frac{(T/\tilde{T})^{4n}}{1+2(T/\tilde{T})^{2n}} \tag{22}$$

and

$$T_\Phi(\Phi) = \tilde{T}\left[e^{\frac{2n\Phi}{\sqrt{3}}} + \sqrt{e^{\frac{2n\Phi}{\sqrt{3}}} + e^{\frac{4n\Phi}{\sqrt{3}}}}\right]^{\frac{1}{2n}}. \tag{23}$$

With the parameters $\tilde{T} = 1.08\,T_c$ and $n = 6$ the function (21) well approximates the lattice results I and II in the region

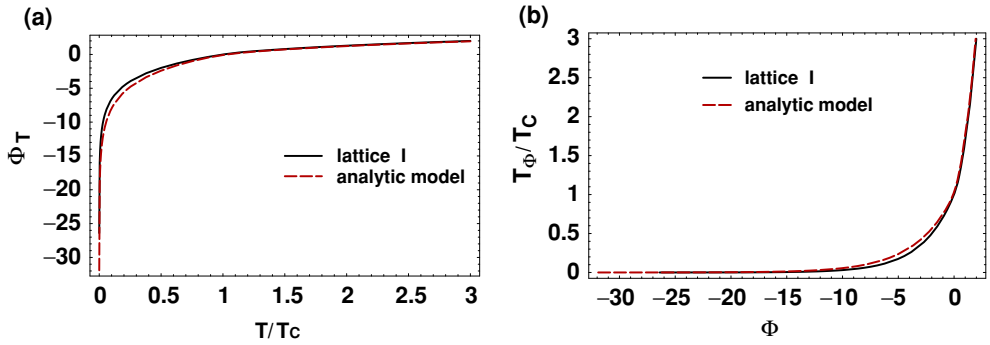

FIG. 2. (Color online) (a) The potential Φ obtained by the integration of Eq. (13). (b) Temperature as a function of the potential Φ. In both cases the solid lines show the results obtained with the lattice equation of state, whereas the dashed lines describe the analytic model defined by Eq. (21).

slightly above T_c and falls between the lattice results I and II at higher temperatures. At low temperatures, $T < 0.6\,T_c$, the function (21) behaves like a constant [see Fig. 1(b)]. The functions $\Phi_T(T)$ and $T_\Phi(\Phi)$, defined by Eqs. (22) and (23) with $\tilde{T} = 1.08\,T_c$ and $n = 6$, are represented in Fig. 2 by the dashed lines. The solid lines in Fig. 2 show the same functions obtained for the lattice case. *In the following, we shall refer to the lattice calculations having in mind the lattice I case, including a linear extrapolation at very low temperatures.*

We note that our two choices of the sound velocity function $c_s(T)$ satisfy the condition for the stability of the solutions against shock formation [12,51]:

$$1 - c_s^2 + c_s T \frac{dc_s}{dT} = \frac{c_s T^2}{\sigma} \frac{d}{dT}\left(\frac{\sigma c_s}{T}\right) \geqslant 0. \tag{24}$$

If the sound velocity decreases suddenly as a function of temperature, as is the case during the first-order phase transition or very rapid crossover transitions, the hydrodynamic solutions develop a shock. In this situation our method of solving the hydrodynamic equations no longer applies. Fortunately, a decrease of the sound velocity with temperature shown in the Fig. 1(a) in the resonance gas region $0.5T_c < T < T_c$ is moderate and does not lead to shock instabilities. Moreover, the relatively low value of c_s in the region below the phase transition satisfies the necessary condition for the development of scaling solutions at large times during three-dimensional expansion [10,22]:

$$c_s^2 \leqslant \frac{1}{5}. \tag{25}$$

IV. INITIAL CONDITIONS

For symmetry reasons, the velocity field should vanish at $r = 0$. This condition is achieved if the functions a_+ and a_- are initially determined by a single function $a(r)$ according to the prescription [12]

$$a_+(t = t_0, r) = a(r), \quad a_-(t = t_0, r) = a(-r). \tag{26}$$

In the following we shall assume that the hydrodynamic evolution starts at a typical time $t = t_0 = 1$ fm. We shall also assume that the initial temperature profile is connected with the nucleon-nucleus thickness function $T_A(r)$,

$$T(t = t_0, r) = (\text{constant})\, T_A^{1/3}(r), \tag{27}$$

where

$$T_A(r) = 2 \int dz\, \rho\left(\sqrt{r^2 + z^2}\right). \tag{28}$$

Here the function $\rho(r)$ is the nuclear density profile given by the Woods-Saxon function with a conventional choice of the parameters [$\rho_0 = 0.17\,\text{fm}^{-3}$, $r_0 = (1.12A^{1/3} - 0.86A^{-1/3})\,\text{fm}$, $a = 0.54\,\text{fm}$, $A = 197$]. The idea of using Eq. (27) follows from the assumption that the initially produced entropy density $\sigma(r)$ is proportional to the number of nucleons participating in the collision at a distance r from the collision center [19], $\sigma(r) \sim T_A(r)$. Since for massless particles the entropy density is proportional to the third power of the temperature, we arrive at Eq. (27).

We note that other choices for the initial temperature profile are also conceivable. If we assume that the initially produced energy density is proportional to the nuclear thickness function, instead of Eq. (27) we obtain

$$T(t = t_0, r) = (\text{constant})\, T_A^{1/4}(r). \tag{29}$$

We checked, however, that the change of the power from 1/3 in Eq. (27) to 1/4 in Eq. (29) does not affect our results (this point will be illustrated later). If we assume that the energy deposition into the thermalization is driven by the collisions of wounded nucleons, and every collision contributes with certain probability distribution to a local increase in temperature, then after many collisions the central limit theorem may describe the form of the local temperature distribution and this is a Gaussian. However, if there are substantial fluctuations in the deposited energy, the generalized central limit theorems apply and in this case the local temperature distribution may have the generalized, Lévy stable form. As a special case, the Lorentzian temperature profile can also be obtained.

The two initial conditions (6) and (27) may be included in the initial form of the function $a(r)$ if we define

$$a(t = t_0, r) = a_T(r) \frac{\sqrt{1 + v_r^0}}{\sqrt{1 - v_r^0}}, \tag{30}$$

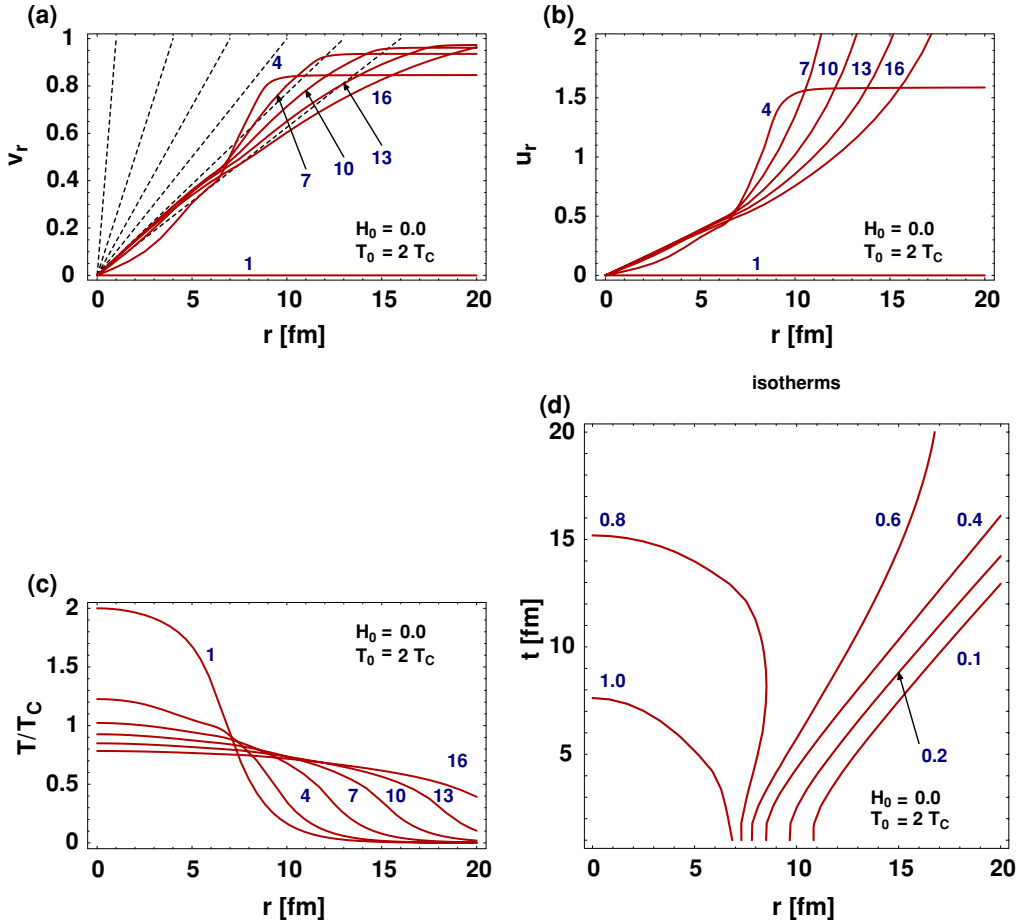

FIG. 3. (Color online) Hydrodynamic expansion of matter being initially at rest (i.e., in the case $H_0 = 0$). The initial central temperature $T_0 = 2T_c$. (a) The transverse velocity as a function of the distance from the center for six different values of time, $t_i = 1,\ 4,\ 7,\ 10,\ 13$, and 16 fm. The dashed thin lines describe the ideal Hubble-like profiles of the form r/t_i ($r < t_i$). (b) The transverse four-velocity as a function of r for the same values of time. (c) The temperature profiles in r. (d) Isotherms in t–r space. In this case, the labels at the curves denote the values of the temperature in units of the critical temperature.

where

$$a_T(r) = \exp\left[\Phi_T\left((\text{constant})\, T_A^{\frac{1}{3}}(|r|)\right)\right]. \qquad (31)$$

V. RESULTS

It is important to observe that the Hubble law $v = Hr$ is satisfied in the $r \ll t$ region after $t = 7$ fm in all the cases we explored numerically in the present calculation, regardless of the initial conditions. However, the value of the Hubble constant typically deviates from the inverse of time, which signals that the asymptotic form of the Hubble flow, Eq. (3), is reached only after a longer time period. The onset of the asymptotic scaling is determined by the initial conditions as we shall detail in the following.

In Figs. 3 and 4 we show our results obtained for two different initial conditions characterized by the two different initial values of the parameter H_0, $H_0 = 0$ and $H_0 = 0.25\,(\text{fm}/c)^{-1}$, respectively. In both cases the lattice equation of state is used and the initial temperature in the center of the system is assumed to be twice the temperature of the phase transition, $T_0 = T(t = t_0, r = 0) = 2T_c$. This means that, for the commonly accepted value of T_c, which is about 170 MeV, the initial temperature in the center reaches about 340 MeV.

In the $H_0 = 0$ case, the transverse flow is initially set to zero but it builds up during the evolution of the system, as shown in Fig. 3(a). The corresponding values of the transverse four-velocity u_r are plotted in the Fig. 3(b). To check whether the flow approaches the asymptotic scaling solution, we compare the velocity profiles calculated numerically at different times $t_i = 1, 4, 7, 10, 13$, and 16 fm (solid lines) with the ideal Hubble-like velocities of the form r/t_i (thin dashed lines) in the regions $r < t_i$. As expected, in the $H_0 = 0$ case the calculated profiles do not agree with the ideal curves in the considered evolution times.

In Fig. 3(c) we observe that the central part of the system cools down very quickly from $T = 2T_c$ to the critical temperature $T = T_c$ and subsequent cooling is much slower.

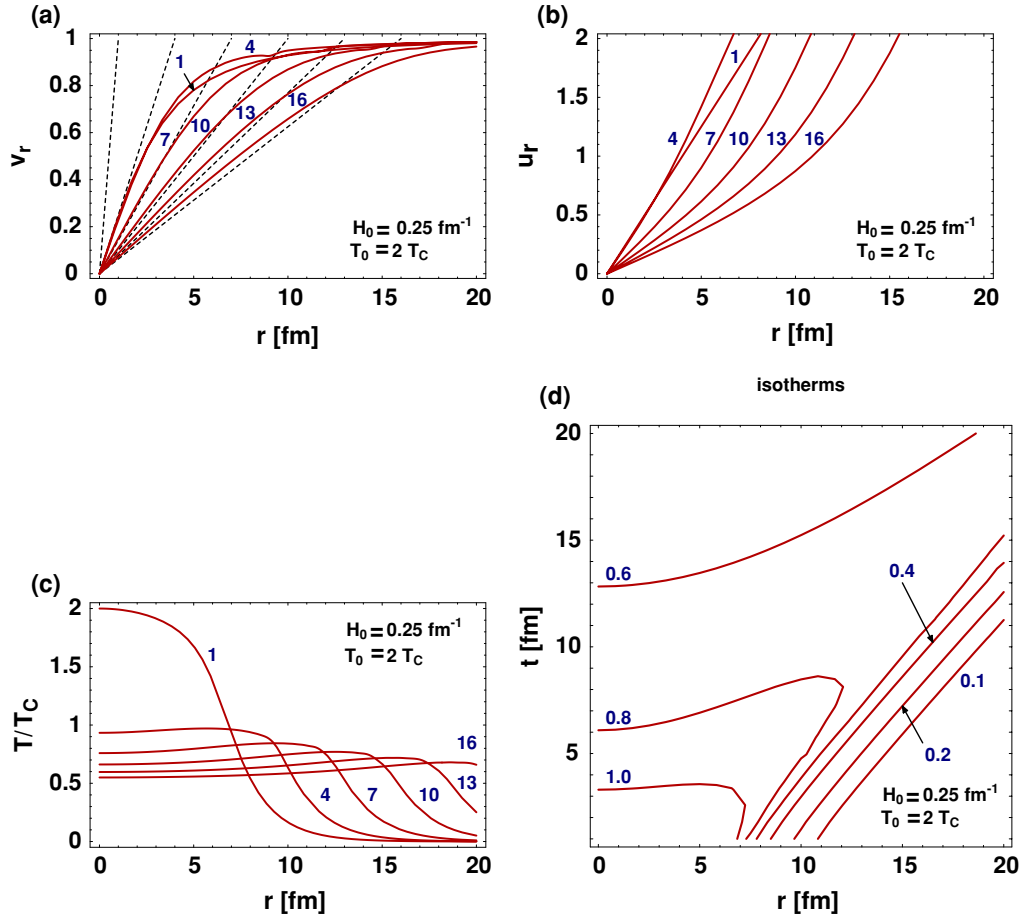

FIG. 4. (Color online) Hydrodynamic expansion of matter with initial pre-equilibrium flow characterized by the velocity profile (6) with $H_0 = 0.25\,\mathrm{fm}^{-1}$. The initial central temperature $T_0 = 2T_c$. Notation as in Fig. 3.

This behavior is caused by different values of the sound velocity in the regions above and below T_c; larger values of c_s in the plasma phase imply its faster cooling. We note that for the first-order phase transition the speed of sound drops to zero at $T = T_c$ and the system keeps on expanding at a constant temperature of $T = T_c$. In the present case we deal with a sudden crossover transition, hence the expansion in volume is coupled to a small decrease in temperature. From Fig. 3(d) showing the isotherms in the t–r space, we may conclude that expansion of the system without noticeable cooling below T_c takes longer than 15 fm.

The evolution of matter shown in Fig. 3 may be compared with the situation where the nonzero pre-equilibrium flow is included in the initial condition. In Fig. 4 we show our results obtained in the $H_0 = 0.25\,(\mathrm{fm}/c)^{-1}$, case with the same initial central temperature $T_0 = 2T_c$. Since the transverse flow is already present at the beginning of the evolution, the expansion of the system is much faster than that discussed in the previous case of $H_0 = 0$. In Fig. 4(a) we show the velocity profiles in r, again for six different values of time. By comparing these to the ideal curves of the form r/t_i (thin dashed lines) we observe that the flow approaches the asymptotic scaling solution after about 7 fm.

In Fig. 4(c) we can see similar behavior to that presented in Fig. 3(c), namely, the initial fast cooling of the hot center, which slows down when the system approaches T_c. We observe, however, that in the $H_0 = 0.25\,(\mathrm{fm}/c)^{-1}$ case the slowdown of the cooling process is not as effective as that observed in the $H_0 = 0$ case. Because of the larger transverse flow, the energy from the interior is transported outside, the temperature in the center continues to drop, and a very interesting situation happens: Parts of the system away from the center become hotter than the center, when different positions are compared at the same time in the lab. However, when different positions are compared at the same proper time, the surface is a little bit colder than the center, as shown in Fig. 4(d). We note that isotherms of similar shape are used in the Cracow model where they are defined by the condition of constant proper time τ [2]. The blast-wave model assumes that freeze-out happens at a constant value of the ordinary time t with a fixed temperature T, whereas the Buda-Lund model assumes that the temperature profile may eventually decrease to 0 at large transverse extensions, hence capturing the feature that the temperature vanishes for very large transverse coordinates in all of the presented calculations.

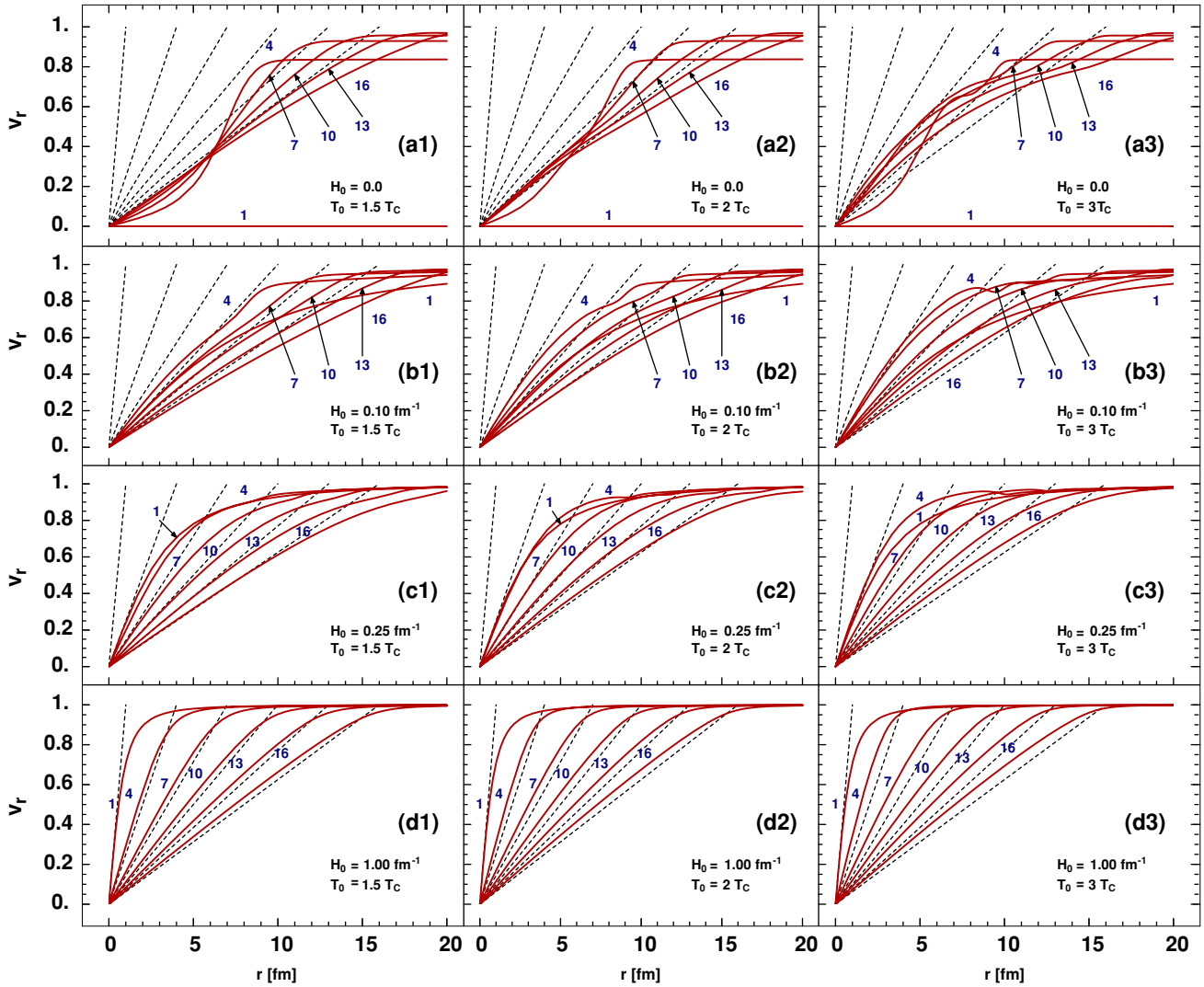

FIG. 5. (Color online) Velocity profiles in r (solid lines) calculated for different initial values of the Hubble constant H_0 and different initial values of the central temperature T_0. The labels 1, 4, 7, 10, 13, and 16 denote the evolution time in fm. The thin dashed lines show the ideal profiles of the form r/t obtained for the same values of time.

In Fig. 5 we show a collection of velocity profiles obtained for four different initial values of the Hubble constant H_0 and for three different initial values of the central temperature T_0. The four rows of smaller figures describe the results obtained with $H_0 = 0.0$, 0.10, 0.25, and $1.0\,(\mathrm{fm}/c)^{-1}$; the three columns correspond to the central temperature $T_0 = 1.5T_c$, $T_0 = 2T_c$, and $T_0 = 3T_c$.

The results presented in Fig. 5 are obtained with the analytic model for the temperature dependence of the sound velocity, hence, by comparison of Fig. 5 with the two previous figures, the effects of the change of the function $c_s(T)$ on the time evolution of the system may be observed. For example, comparing Fig. 5(c2) with Fig. 4(a) [both results obtained with $H_0 = 0.25\,(\mathrm{fm}/c)^{-1}$ and $T_0 = 2T_c$] we can see that the flow obtained with the analytic model is closer to the asymptotic scaling form than the flow obtained for the lattice equation of state. We note that the main difference between the two cases is that the sound velocity in the analytic model is lower in the hadronic phase. The asymptotic scaling solutions are more easily generated at the reduced values of the sound velocity, as shown in Refs. [10,24,25]. This effect explains the better agreement of the generated transverse flow with the asymptotic scaling solution obtained in the analytic model.

Let us now discuss the impact of the initial temperature distribution on the formation of the transverse flow. Since the spatial extension of the system is the same in all considered cases (roughly the diameter of a gold nucleus), a higher initial central temperature implies a larger pressure gradient, leading directly to the formation of the stronger flow. This effect is seen in Fig. 5 if the results obtained with the same initial value of the flow parameter H_0 but different initial values of the central temperature T_0 are compared. The presence of the pre-equilibrium transverse flow helps to develop the strong transverse flow, and this effect is added to the effects of the pressure gradient. This is clearly seen in the case $H_0 = 0.10\,(\mathrm{fm}/c)^{-1}$, depicted in Figs. 5(b1)–5(b3). At $t =$ 16 fm the flow in the range $r < 10$ fm is close but below the

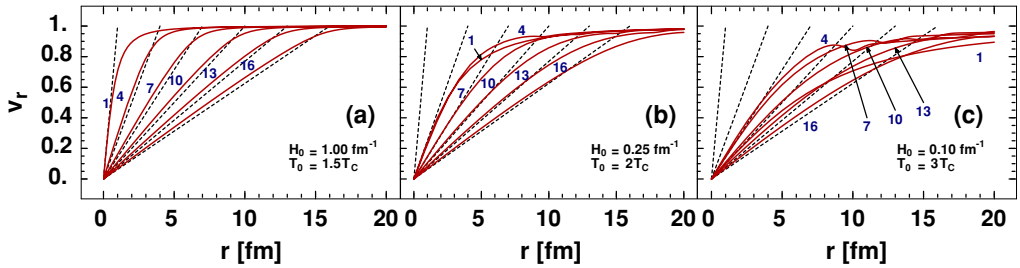

FIG. 6. (Color online) Three examples of the velocity profiles in r obtained for the initial conditions specified by Eq. (29).

asymptotic scaling solution for $T_0 = 2T_c$ and close but above the asymptotic scaling solution for $T_0 = 3T_c$. For $T_0 = 1.5T_c$ the flow is noticeably below the asymptotic scaling form. We conclude that the asymptotic solution may be reached either from above or from below (in the region $r \ll t$), depending on the value of the initial temperature. For a fixed value of T_0, the asymtotic solution is approached from above, if the pre-equilibrium flow is sufficiently strong. This behavior is indicated by our results obtained for $H_0 = 0.25\,(\mathrm{fm}/c)^{-1}$ and $H_0 = 1.0\,(\mathrm{fm}/c)^{-1}$ [Figs. 5(c1)–5(d3)]. Interestingly, in the case $H_0 = 1/t_0 = 1.0\,(\mathrm{fm}/c)^{-1}$, where the initial flow agrees with the scaling form already at the beginning of the time evolution, the pressure gradient accelerates the matter and the convergence to the scaling form is delayed, if $T_0 \geqslant 2T_c$.

In any case, the existence of a nonzero pre-equilibrium flow seems to be a necessary condition for the formation of the accelerationless Hubble-like flows in the evolution times of 10–15 fm. This is indicated by our results obtained with $H_0 = 0$ for different values of T_0 [Figs. 5(a1)–5(a3)]. The amount of pre-equilibrium flow required to achieve the fast convergence to the asymptotic solution depends on the initial temperature (pressure gradient); smaller initial values of the Hubble constant H_0 may be compensated by larger initial values of the central temperature T_0. For example, at $t = 16$ fm the flow profiles are very similar in the following cases: $H_0 = 1\,(\mathrm{fm}/c)^{-1}$ and $T = 1.5T_0$ [Fig. 5(d1)], $H_0 = 0.25\,(\mathrm{fm}/c)^{-1}$ and $T = 2T_c$ [Fig. 5(c2)], and $H_0 = 0.1\,(\mathrm{fm}/c)^{-1}$ and $T = 3T_c$ [Fig. 5(b3)]. The asymptotic Hubble flow is reached by about 7–10 fm in Fig. 5(b3), whereas the same form is reached by about 4–7 fm in Fig. 5(c2) and 1–4 fm in Fig. 5(d1).

In Ref. [52] hydrodynamic calculations were done with zero initial transverse flow but very large initial temperature, $T_0 = 2$ GeV. In this case the isotherms have similar features to those shown in Fig. 4(d), suggesting formation of a very strong (possibly scaling) transverse flow. It is quite remarkable that the presence of the pre-equilibrium flow is required only to set the value of the Hubble constant to $H = 1/t$, that is, to reach the scaling solution within a short time period; however, we find that the linear flow profiles, $v = H_0 r$, develop with $H_0 \neq 1/t$ in all the considered cases by about 7 fm, regardless of the details of the initial conditions.

Finally, in Fig. 6 we show the flow profiles obtained for the initial thermal distributions obtained from Eq. (29). By comparison of the results presented in the three parts of Fig. 6 with the corresponding three parts of Fig. 5 (with the same values of H_0 and T_0) we conclude that the change of the power in the relation between the temperature and the thickness function from 1/3 to 1/4 is insignificant for the outcome of the numerical calculations.

VI. CONCLUSIONS

Our results show the dynamical development of scaling solutions in relativistic hydrodynamics applied to relativistic heavy-ion collisions. We considered realistic initial conditions that connect the entropy density of the initial state with the number of participating nucleons. If the initial values of the Hubble constant H_0 and the central temperature T_0 are covaried in a reasonable range, a Hubble-type, linear transverse flow $v = Hr$ develops after 7 fm. However, it is more difficult for the transverse flow to achieve its *asymptotic*, accelerationless scaling form, that is, to reach the time dependence of $H(t) = 1/t$, by the evolution time of about 7–15 fm.

The necessary conditions to reach the corresponding asymptotic form of $v = r/t$ are thus threefold: (1) The lattice QCD equation of state has to be used, with the corresponding temperature-dependent speed of sound. This generates very strong transverse flows within the short time scales suggested by the phenomenological analysis of the experimental data of Au + Au collisions at RHIC. (2) Pre-equilibrium transverse flow has to already be present at the beginning of the hydrodynamic evolution, that is, at the initial time of about 1 fm. (3) The precise amount of the requisite pre-equilibrium flow is anticorrelated with the initial value of the central temperature, because for larger initial pressure gradients, smaller initial flows are necessary.

Using such anticorrelated initial conditions and a lattice QCD equation of state, the numerical solutions of relativistic hydrodynamics are shown to reproduce qualitatively key features of the blast-wave, Buda-Lund, and Cracow models. More detailed investigations are necessary to explore these relationships on the quantitative level.

ACKNOWLEDGMENTS

This work was supported in part by the Polish State Committee of Scientific Research, Grant 2 P03B 05925, by the Hungarian OTKA Grant T038406, by the MTA–OTKA–NSF Grant INT0089462, and by the exchange program of the Hungarian and Polish Academy of Sciences as well as by the Polish KBN–Hungarian Ministry of Education Exchange Programme in Science and Technology.

[1] QM02, Nucl. Phys. **A715**, Proceedings of the 16th International Conference on Ultra-Relativistic Nucleus-Nucleus Collisions (Nantes, France, 2003).
[2] W. Broniowski and W. Florkowski, Phys. Rev. Lett. **87**, 272302 (2001).
[3] W. Broniowski and W. Florkowski, Phys. Rev. C **65**, 064905 (2002).
[4] M. Csanád, T. Csörgö, B. Lörstad, and A. Ster, J. Phys. G **30**, S1079 (2004).
[5] J. Allday, *Quarks, Leptons and the Big Bang* (Institute of Physics Publishing, Bristol and Philadelphia, 2002).
[6] J. P. Bondorf, S. I. A. Garpman, and J. Zimányi, Nucl. Phys. **A296**, 320 (1978).
[7] L. D. Landau, Izv. Akad. Nauk. SSSR Ser. Fiz. **17**, 51 (1953).
[8] S. Z. Belenkij and L. D. Landau, Nuovo Cimento (Suppl.) **3S10**, 15 (1956).
[9] F. Cooper, G. Frye, and E. Schonberg, Phys. Rev. Lett. **32**, 862 (1974).
[10] F. Cooper, G. Frye, and E. Schonberg, Phys. Rev. D **11**, 192 (1975).
[11] J. D. Bjorken, Phys. Rev. D **27**, 140 (1983).
[12] G. Baym, B. L. Friman, J. P. Blaizot, M. Soyeur, and W. Czyz, Nucl. Phys. **A407**, 541 (1983).
[13] R. C. Hwa, Phys. Rev. D **10**, 2260 (1974).
[14] C. B. Chiu and K.-H. Wang, Phys. Rev. D **12**, 272 (1975).
[15] C. B. Chiu, E. C. G. Sudarshan, and K.-H. Wang, Phys. Rev. D **12**, 902 (1975).
[16] M. I. Gorenstein, Y. M. Sinyukov, and V. I. Zhdanov, Phys. Lett. **B71**, 199 (1977).
[17] M. I. Gorenstein, Y. M. Sinyukov, and V. I. Zhdanov, Zh. Eksp. Teor. Fiz. [Sov. Phys.—JETP] **74**, 833 (1978).
[18] P. Huovinen, Acta Phys. Pol. B **33**, 1635 (2002).
[19] P. F. Kolb and U. Heinz, nucl-th/0305084.
[20] D. Teaney, J. Lauret, and E. V. Shuryak, nucl-th/0110037.
[21] T. Hirano, J. Phys. G **30**, S845 (2004).
[22] J. Y. Ollitrault, Phys. Rev. D **46**, 229 (1992).
[23] M. Kataja, P. V. Ruuskanen, L. D. McLerran, and H. von Gersdorff, Phys. Rev. D **34**, 2755 (1986).
[24] T. S. Biro, Phys. Lett. **B474**, 21 (2000).
[25] T. S. Biro, Phys. Lett. **B487**, 133 (2000).
[26] T. Csörgö, F. Grassi, Y. Hama, and T. Kodama, Heavy Ion Phys. A **21**, 53 (2004).
[27] T. Csörgö, F. Grassi, Y. Hsama, and T. Kodama, Heavy Ion Phys. A **21**, 63 (2004).
[28] T. Csörgö, F. Grassi, Y. Hama, and T. Kodama, Phys. Lett. **B565**, 107 (2003).
[29] T. Csörgö, L. P. Csernai, Y. Hama, and T. Kodama, Heavy Ion Phys. A **21**, 73 (2004).
[30] F. Retiere and M. A. Lisa, Phys. Rev. C **70**, 044907 (2004).
[31] F. Retiere, J. Phys. G **30**, S827 (2004).
[32] A. N. Makhlin and Y. M. Sinyukov, Z. Phys. C **39**, 69 (1988).
[33] T. Renk, Phys. Rev. C **69**, 044902 (2004).
[34] M. Csanád, T. Csörgö, B. Lörstad, and A. Ster, nucl-th/0402037.
[35] P. F. Kolb and R. Rapp, Phys. Rev. C **67**, 044903 (2003).
[36] S. V. Akkelin, T. Csörgö, B. Lukács, Y. M. Sinyukov, and M. Weiner, Phys. Lett. **B505**, 64 (2001).
[37] T. Csörgö, Cent. Eur. J. Phys. **2**(4), 556 (2004); nucl-th/9809011.
[38] T. Csörgö, S. V. Akkelin, Y. Hama, B. Lukács, and Y. M. Sinyukov, Phys. Rev. C **67**, 034904 (2003).
[39] I. G. Bearden *et al.* (BRAHMS), Phys. Rev. Lett. **90**, 102301 (2003).
[40] I. G. Bearden (BRAHMS), nucl-ex/0403050.
[41] W. Florkowski, W. Broniowski, and M. Michalec, Acta Phys. Pol. B **33**, 761 (2002).
[42] G. Torrieri, S. Steinke, W. Broniowski, W. Florkowski, J. Letessier, and J. Rafelski, nucl-th/0404083.
[43] B. Mohanty and J.-E. Alam, Phys. Rev. C **68**, 064903 (2003).
[44] F. Karsch, Nucl. Phys. **A698**, 199 (2002).
[45] K. K. Szabó and A. I. Tóth, J. High Energy Phys. **6**, 8 (2003).
[46] W. Broniowski and W. Florkowski, Phys. Lett. **B490**, 223 (2000).
[47] W. Broniowski, hep-ph/0008112.
[48] W. Broniowski, W. Florkowski, and L. Y. Glozman, Phys. Rev. D **70**, 117503 (2004).
[49] R. Hagedorn, Nuovo Cimento (Suppl.) **3**, 147 (1965).
[50] D. Prorok, Acta Phys. Pol. B **33**, 1583 (2002).
[51] J. P. Blaizot and J. Y. Ollitrault, Phys. Lett. **B191**, 21 (1987).
[52] U. Heinz and P. F. Kolb, Phys. Lett. **B542**, 216 (2002).